

## ARTICLE TYPE

# Dynamically Adaptive FAS for an Additively Damped AFAC Variant<sup>†</sup>

Charles D. Murray\* | Tobias Weinzierl

<sup>1</sup>Department of Computer Science, Durham University, Durham, United Kingdom**Correspondence**

\*Charles Murray, Department of Computer Science, Durham University, Durham, United Kingdom. Email: c.d.murray@durham.ac.uk

**Abstract**

Multigrid solvers face multiple challenges on parallel computers. Two fundamental ones are that multiplicative solvers issue coarse grid solves which exhibit low concurrency and that many multigrid implementations suffer from an expensive coarse grid identification phase as well as dynamic adaptive mesh refinement (AMR) overhead. We therefore propose a new additive variant of the fast adaptive composite (FAC) method which can be combined with Full Approximation Storage (FAS) plus BoxMG inter-grid transfer operators on spacetrees. This allows for a straightforward realisation of arbitrary dynamic AMR on geometric multiscale grids with algebraic operators. The novel flavour of the additive scheme is an augmentation of the solver with an additive, auxiliary damping per grid level that is in turn constructed through the next coarser level—an idea which utilises smoothed aggregation principles or the motivation behind AFACx. This yields improved stability as we experience it with multiplicative schemes, while pipelining techniques help us to write down the additive solver with single-touch semantics.

**KEYWORDS:**

adaptive mesh refinement, additive multigrid, full approximation storage, BoxMG, smoothed aggregation, asynchronous FAC, single-touch

## 1 | INTRODUCTION

The elliptic partial differential equation (PDE)

$$-\nabla(\epsilon \nabla)u = f, \quad \epsilon : \Omega \subset \mathbb{R}^d \mapsto \mathbb{R}^+ \text{ either constant or varying} \quad (1)$$

serves as building block in many applications. Examples are chemical dispersion in sub-surface reservoirs, the heat distribution in buildings, or the diffusion of oxygen in tissue. It is also the starting point to construct more complex differential operators. Solving this PDE quickly is important yet not trivial. One reason is buried within the operator: any local modification of the solution propagates among the whole computational domain unless damped out, i.e. effectively stopped, due to large  $\epsilon$  variations. The operator exhibits multiscale behaviour. A successful family of iterative techniques to solve (1) hence is multigrid. It relies on representations of the operator's behaviour on multiple scales. It builds the operator's multiscale behaviour into the algorithm.

There are conceptional, algorithmic and implementational hurdles that must be tackled when we write multigrid codes. In this paper, we focus on three conceptual challenges which should be addressed before we scale up multigrid. (i) If an algorithm solves problems on cascades of coarser and coarser, i.e. smaller and smaller, problems, the smallest problems eventually do

<sup>†</sup>The work was funded by a Durham University/EPSRC DTA PhD scholarship. It made use of the facilities of the Hamilton HPC Service of Durham University.

not exhibit enough computational work to scale among larger core counts. (ii) State-of-the-art multigrid codes have to support dynamically adaptive mesh refinement (AMR) without significant overhead. While constructing coarser (geometric) representations from regular grids is straightforward, it is non-trivial for adaptive meshes. (iii) If an algorithm projects a problem to multiple resolutions and then constructs a solution from these resolutions, its implementation tends to read and write data multiple times. Repeated data access however is poisonous on today’s hardware which suffers from a widening gap between what cores could compute and what throughput memory can provide<sup>1</sup>.

We propose a solver-implementation combination which tackles the challenges in one rush. It combines several state-of-the-art building blocks. Our first algorithmic block is the spacetree paradigm, a generalisation of the classic octree/quadtree idea<sup>2,3</sup>. Spacetrees yield adaptive Cartesian grids which are nested within each other<sup>2-5</sup>. Adaptivity decreases the cost of a solve by reducing the degrees of freedom without adversely affecting the accuracy. It invests work where it pays off. With complex boundary conditions or non-trivial  $\epsilon$ —or even  $\epsilon(u)$  which renders (1) nonlinear—the regions where to refine are not known a priori. Schemes that allow for dynamic mesh refinement are therefore key for many applications. Our second algorithmic building block is additive multigrid. Additive multigrid exhibits greater parallelism than multiplicative multigrid, as different levels are computed independently of each other. There is no close-to-serial coarse grid solve. Our third algorithmic building block is the triad of fast adaptive composite (FAC), hierarchical transformation multigrid (HTMG)<sup>6</sup> and full approximation storage (FAS)<sup>7</sup>. These three techniques allow us to elegantly realise a multigrid scheme which straightforwardly works for dynamically adaptive meshes. Fourth, it unfolds its full potential once we merge it with quasi matrix-free multigrid relying on algebraic BoxMG inter-grid transfer operators<sup>5,8,9</sup>. Our last algorithmic building block is pipelining combined with recursive element-wise grid traversals. We run through the spacetree depth-first which yields excellent cache hit rates<sup>2</sup> and simple recursive implementations. The approach equals a multiscale element-wise grid traversal. Going from coarse levels to fine levels and backtracking however does not fit straightforwardly to FAS with additive multigrid, where we restrict the residual from fine to coarse, prolong the correction from coarse to fine and inject the solution from fine to coarse again. Yet, we know that some additional auxiliary variables allow us to write additive solvers single-touch<sup>4</sup>. Each unknown is read into the chip’s caches once per cycle.

Due to its reduced synchronisation and the absence of isolated small-scale solves, the additive mindset is promising for the era of massive concurrency growth<sup>1</sup>. Notably recent work on a further decoupling of both the individual levels’ solves as well as the solves within a level<sup>10</sup> shows great upscaling potential. However, plain additive approaches face a severe problem. They are less robust. Naïvely restricting residuals to multiple levels and eliminating errors concurrently tends to make the iterative scheme overshoot<sup>10,11</sup>. Multiple strategies exist to improve the stability without compromising on the additivity. In the simplest case, we merely employ additive multigrid as a preconditioner and use a more robust solver thereon. Our work goes down the “multigrid as a solver” route: A well-known approach to mitigate overshooting in the solver is to damp levels the more aggressively the coarser they are. This reduces their impact and improves stability but decreases the rate of convergence<sup>4</sup>. We refrain from such resolution-parameterised damping and follow up on the idea behind AFACx<sup>12-15</sup>: By introducing an additional solution component per level, our approach predicts additive overshooting from coarser levels. Different to AFACx, we however do not make the additional auxiliary solves preprocessing steps. We phrase them completely parallel (additive) to the actual correction’s solve. To make the auxiliary contributions meaningful nevertheless, we tweak them through ideas resembling smoothed aggregation<sup>16-18</sup> which approximate the smoothing steps of multiplicative multigrid<sup>19</sup>. We end up with an *additively damped Asynchronous FAC* (adAFAC). Our adAFAC implementation merges the levels of the multigrid scheme plus their traversal into each other, and thus provides a single-touch implementation. Through this, we eliminate synchronisation between the solves on different resolution levels and anticipate that FAC yields multigrid grid sequences where work non-monotonously grows and shrinks upon each resolution transition. We vertically integrate solves<sup>20</sup> and make domain decomposition a spatial, single-level challenge again.

We reiterate which algorithmic ingredients we use in Section 2 before we introduce our new additive solver adAFAC (Section 3). Section 4 then translates adAFAC into a single-touch algorithm blueprint. Some numerical results uncover the solver’s potential (Section 5), after which we close the discussion with a brief summary and sketch future work.

## 2 | RELATED WORK AND METHODOLOGICAL INGREDIENTS

### 2.1 | Spacetrees

Our meshing relies upon a spacetree<sup>2,3</sup> (Figure 1): The computational domain is embedded into a square ( $d = 2$ ) or cube ( $d = 3$ ) which yields a (degenerated) Cartesian mesh with one cell and  $2^d$  vertices. We use cell as generic synonym for cube or

square, respectively. Let the bounding cell have level  $\ell = 0$ . It is equidistantly cut into  $k$  parts along each coordinate axis. We obtain  $k^d$  child cells having level  $\ell = 1$ . The construction continues recursively while we decide per cell individually whether to refine further or not. The process creates a cascade of Cartesian grids  $\Omega_{\ell=0}, \Omega_{\ell=1}, \Omega_{\ell=2}, \dots$ . We count levels the other way round compared to most multigrid literature<sup>7, 21</sup>. They make the finest grid hold level  $\ell = 0$  and assign increasing indices from fine to coarse. Our level grids might be ragged:  $\Omega_\ell$  is a regular grid covering the whole domain if and only if all cells on all levels  $\hat{\ell} < \ell$  are refined. We use  $k = 3$ . Choosing three-partitioning is due to<sup>2, 3</sup> acting as implementation baseline. All of our concepts however apply to bipartitioning, too.

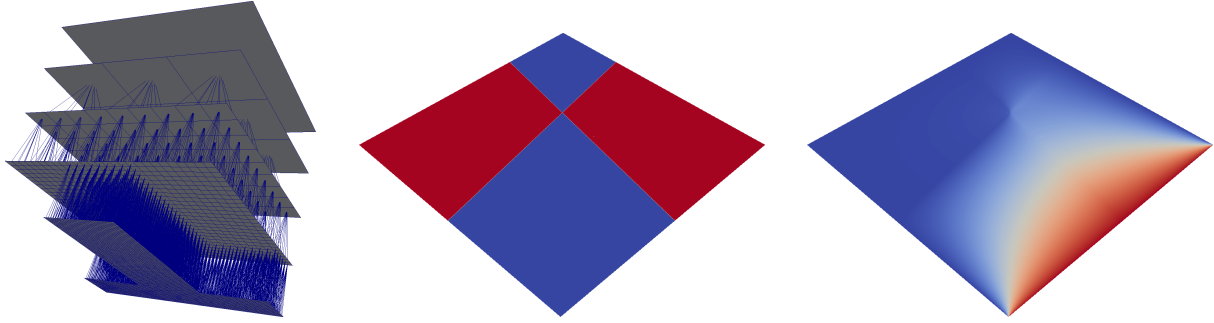


**FIGURE 1** Left: A  $3 \times 3$  mesh ( $\ell = 1$ ; top layer) serves as first refinement level. From here, we construct subsequent refinement levels by subdividing cells into  $3 \times 3$  patches. This yields a spacetime. Multiple Cartesian meshes are embedded into each other. Middle: Conductivity (material) parameter setup as used for a stationary heat equation solve where the right bottom side of the unit square is heated up. A high conductivity in two domain subregions makes the solution (right) asymmetric.

Our code discretises (1) with  $d$ -linear Finite Elements. Each vertex on each level  $\ell$  that is surrounded by  $2^d$  cells on level  $\ell$  carries one “pagoda”, i.e. bi- or tri-linear shape function. The remaining vertices are hanging vertices. Testing shape functions against other functions from the same level yields compact  $3^d$  stencils. For this, we make hanging and boundary vertices carry truncated shape functions but no test functions. A discussion of Neumann conditions is out of scope. We therefore may assume that the scaling of the truncated shapes along the boundary is known. Due to the spacetime’s construction pattern, stencils act on a nodal generating system over an adaptive Cartesian grid  $\Omega_h = \cup_\ell \Omega_\ell$ . If we study (1) only over the vertices from all levels that carry a shape function and do not spatially coincide with any other vertex of the grid from finer levels, we obtain a nodal shape space over an adaptive Cartesian grid  $\Omega_h$ .

Let  $\ell_{\max}$  identify the finest mesh, i.e. the maximum level, while  $\ell_{\min} \geq 1$  is the coarsest level which holds degrees of freedom.  $\ell_{\max} \geq \ell_{\min}$ . Usually,  $\ell_{\min} = 1$  is appropriate, though experience teaches us that bigger  $\ell_{\min}$  might be reasonable if a problem’s solution can’t be accurately represented on the coarsest meshes anymore. Our subsequent discussion introduces the linear algebra ingredients for a regular grid corresponding to  $\ell_{\max}$ . The elegant handling of the adaptive grid is subject of a separate subsection where we exploit the transition from a generating system into a basis. Without loss of generality, (1) is thus discretised into

$$A_{\ell_{\max}} u_{\ell_{\max}} = b_{\ell_{\max}}.$$

## 2.2 | Additive and multiplicative multigrid

Additive multigrid reads as

$$u_{\ell_{\max}} \leftarrow u_{\ell_{\max}} + \left( \sum_{\ell=\ell_{\min}}^{\ell_{\max}} \omega_{add}(\ell) P^{\ell_{\max}-\ell} M_\ell^{-1} R^{\ell_{\max}-\ell} \right) (b_{\ell_{\max}} - A_{\ell_{\max}} u_{\ell_{\max}}), \quad (2)$$

where  $M_\ell$  is an approximation to  $A_\ell$ . We use the Jacobi smoother  $M_\ell^{-1} = \text{diag}^{-1}(A_\ell)$ . The generic prolongation symbol  $P$  accepts a solution on a particular level  $\ell - 1$  and projects it onto the next finer level  $\ell$ . The exponent indicates repeated application of this inter-grid transfer operator. Restriction works the other way round, i.e. projects from finer to coarser meshes. Ritz-Galerkin multigrid<sup>7</sup> finally yields  $A_\ell = R A_{\ell+1} P$  for  $\ell < \ell_{\max}$ .

For an  $\ell$ -independent, constant  $\omega_{add}(\ell) \in ]0, 1]$ , additive multigrid tends to become unstable once  $\ell_{max} - \ell_{min}$  becomes large<sup>4, 11, 22</sup>: If the fine grid residual  $b_{\ell_{max}} - A_{\ell_{max}} u_{\ell_{max}}$  is homogeneously distributed, the residuals all push the solution into the same direction. Summation of all level contributions then moves the solution too aggressively into this direction. A straightforward fix is exponential damping  $\omega_{add}(\ell) = \hat{\omega}_{add}^{\ell_{max}-\ell}$  with a fixed  $\hat{\omega}_{add} \in ]0, 1[$ . If an adaptive mesh is used,  $\ell_{max} - \ell$  is ill-suited as there is no global  $\ell_{max}$  hosting the solution. We introduce an appropriate, adaptive damping in<sup>4</sup> where we make  $\ell_{max}$  a per-vertex property. It is derived from a tree grammar<sup>23</sup>. Such exponential damping, while robust, struggles to track global solution effects efficiently once many mesh levels are used: The coarsest levels make close to no contribution to the solution.

Multiplicative multigrid is more robust than additive multigrid by construction. Multiplicative multigrid does not make one residual feed into all level updates in one rush, but updates the levels one after another. It starts with the finest level. Before it transits from a fine level into the next coarser level, it runs some approximate solves (smoothing steps) on the current level, and yields a new residual. We may assume that the error represented by this residual is smooth. Yet, the representation becomes rough again on the next level, where we continue to smooth it efficiently. Cascades of smoothers act on cascades of frequency bands. Multiplicative methods are characterised by the number of the pre- and postsmoother steps  $\mu_{pre}$  and  $\mu_{post}$ , i.e. the number of relaxation steps before we move to the next coarser level (pre) or next finer level (post), respectively. The multiplicative multigrid solve closest to the additive scheme is a  $V(0, \mu_{post})$ -cycle, i.e. a scheme without any presmoothing and  $\mu_{post}$  postsmoothing steps. However,  $\mu_{pre} = 0$  yields no classic multiplicative scheme, as the resulting solver does not smooth prior to the coarsening. In practice, it works nevertheless.

We conclude that the  $V(\mu_{pre} = 1, 0)$ -cycle thus is the closest cousin to an additive scheme. The multiplicative two-grid scheme with exact coarse grid solve reads

$$u_{\ell_{max}} \leftarrow PA_{\ell_{max}-1}^{-1} R(b_{\ell_{max}} - A_{\ell_{max}} \left[ u_{\ell_{max}} + \omega_{\ell_{max}} M_{\ell_{max}}^{-1} (b_{\ell_{max}} - A_{\ell_{max}} u_{\ell_{max}}) \right] + \left[ u_{\ell_{max}} + \omega_{\ell_{max}} M_{\ell_{max}}^{-1} (b_{\ell_{max}} - A_{\ell_{max}} u_{\ell_{max}}) \right]). \quad (3)$$

### 2.3 | Multigrid on hierarchical generating systems

Early work on locally adaptive multigrid (see for example<sup>12, 24</sup> as well as the historical notes in<sup>14</sup>) already relies on block-regular Cartesian grids<sup>25</sup> and nests the geometric grid resolutions into each other. The coarse grid vertices spatially coincide with finer vertices where the domain is refined. This yields a hierarchical generating system rather than a basis.

The fast adaptive composite (FAC) method<sup>22, 26</sup> describes a multiplicative multigrid scheme over this hierarchical system: We start from the finest grid, determine the residual equation there, smooth, re-compute the residual and restrict it to the next coarser level. It continues recursively. As we rely on residuals, this is a multigrid scheme. As we smooth and then recompute the residual, it is a multiplicative scheme. Early FAC papers orbit around a small set of reasonable fine grids and leave it open to the implementation which iterative scheme to use. Some explicitly speak of FAC-MG if multigrid is used as the iterative smoother per level. We may refrain from such details and consider FAC as a multiplicative scheme overall which can be equipped with simple single-level smoothers.

The first FAC papers<sup>26</sup> acknowledge difficulties for operators along the resolution transitions. While we discuss an elegant handling of these difficulties in 2.4, FAC traditionally addresses them through a top-down traversal<sup>22</sup>: The cycle starts with the coarsest grid, and then uses the updated solution to impose Dirichlet boundary conditions on hanging nodes on the next finer level. This inversion of the grid level order continues to yield a multiplicative scheme as updates on coarser levels immediately propagate down and as all steps are phrased as residual update equations.

FAC relies on spatial discretisations that are conceptionally close to our spacetrees. Both approaches thus benefit from structural simplicity: As the grid segments per level are regular, solvers (smoothers) for regular Cartesian grids can be (re-)used. As the grid resolutions are aligned with each other, hanging nodes can be assigned interpolated values from the next coarser grid with a geometrically inspired prolongation. As all grid entities are cubes, squares or lines, all operators exhibit tensor-product structure. Through FAC's hierarchical basis approach, it does not share two properties with standard, vanilla multigrid<sup>7</sup> if we encounter adaptive meshes: The fine grid smoothers do not address the real fine grid, but only segments of it having the same resolution. The transition from fine to coarse grid does not imply that the number of degrees of freedom decreases. Rather, the number of degrees of freedom can increase if the finer grid accommodates a very localised AMR region. It is obvious that this poses challenges for parallelisation.

We can mechanically rewrite multiplicative FAC into an additive version. The hierarchical generating system renders this endeavour straightforward. However, plain additive multigrid on a FAC data structure again yields a non-robust, overshooting

solver<sup>4, 22</sup>. There are multiple approaches to tackle this: Additive multigrid with exponential damping removes oscillations at the cost of multigrid behaviour. BPX<sup>21</sup> is the most popular variant where we accept the non-robustness and use the additivity solely as a preconditioner. To make this preconditioner cheap, BPX traditionally neglects (Ritz-Galerkin) coarse grid operators. Instead, it replaces the  $M_\ell^{-1}$  in (2) with a diagonal matrix for the correction equations, where the diagonal matrix is scaled such that it mimics the Laplacian. The hierarchical basis approach starts from the observation that the instabilities within the generating system are induced by spatially coinciding vertices. Therefore, it drops all vertices (and their shape functions) on one level that coincide with coarser vertices. The asynchronous FAC (AFAC) solver family finally modifies the operators to anticipate overshooting. We may read BPX as particular modification of additive multigrid and AFAC as generalisation of BPX<sup>27</sup>.

## 2.4 | HTMG and FAS on spacetrees

Though the implementation of multigrid on adaptive meshes is, in principle, straightforward, implementational complexity arises along resolution transitions. Weights associated to the vertices change their semantics once we compare vertices on a level  $\ell$  which are surrounded by refined spacetree cells to vertices on this level which belong to the fine grid: The latter carry a nodal solution representation, i.e. a scaling of the Finite Element shape functions, while the former carry correction weights. In classic multigrid starting from a fine grid and then traversing correction levels, it is not straightforward how to handle the vertices in-between a fine grid region and a refined region within one level. They carefully have to be separated<sup>4, 5</sup>.

One elegant solution to address this ambiguity relies on full approximation storage (FAS)<sup>7</sup>. Every vertex holds a nodal solution representation. If two vertices  $v_\ell$  and  $v_{\ell+1}$  from two levels spatially coincide, the coarser vertex holds a copy of the finer vertex: In areas where two grids overlap, the coarse grid is the injection  $u_\ell = Iu_{\ell+1}$  of the fine grid. This definition exploits the regular construction pattern of spacetrees. Vertices in refined areas now carry a correction equation equation plus the injected solution rather than a sole correction. The injection couples the fine grid problem with its coarsened representation and makes this representation consistent with the fine grid problem on adjacent meshes which have not been refined further. In the present paper, we use FAS exclusively to resolve the semantic disambiguity that arises for vertices at the boundary between the fine grid and a correction region on one level. Further potential such as  $\tau$ -extrapolation<sup>28</sup> or the application to nonlinear PDEs, i.e.  $\epsilon = \epsilon(u)$  in (1), is not exploited.

Our code relies on HTMG<sup>6</sup> for the implementation of FAS. It also relies on the assumption/approximation that all of our operators can be approximated by Ritz-Galerkin multigrid  $RA_{\ell+1}P = A_\ell$ . Injection  $u_\ell = Iu_{\ell+1}$  allows us to rewrite each and every nodal representation into its hierarchical representation  $\hat{u}_\ell = (id - PI)u_\ell$ . A hierarchical residual  $\hat{r}$  is defined in the expected way. This elegantly yields the modified FAS multigrid equation when we switch from the correction equation to

$$\begin{aligned} A_\ell (u_\ell + c_\ell) &= A_\ell u_\ell + A_\ell c_\ell = R\hat{r}_{\ell+1} \\ &= R(b_{\ell+1} - A_{\ell+1}(u_{\ell+1} - PI_{\ell+1})) = R(b_{\ell+1} - A_{\ell+1}\hat{u}_{\ell+1}), \end{aligned} \quad (4)$$

i.e. per-level equations

$$A_\ell u_\ell = \begin{cases} b_\ell & \text{on the fine grid (regions)} \\ b_\ell = R\hat{r}_{\ell+1} & \text{on the coarse grid (regions) with } \hat{r}_{\ell+1} = b_{\ell+1} - A_{\ell+1}\hat{u}_{\ell+1}. \end{cases}$$

To the smoother,  $u_\ell$  resulting from the injection serves as the initial guess. Subsequently it determines a correction  $c_\ell$ . This correction feeds into the multigrid prolongation.

Equation (4) clarifies that the right-hand side of FAS does not require a complicated calculation: We “simply” have to determine the hierarchical representation  $\hat{u}$  on the finer level, compute a hierarchical residual  $\hat{r}$  on this level (which uses the smoother’s operator), and restrict this value to the coarse grid’s right-hand side.

## 2.5 | BoxMG and algebraic-geometric multigrid hybrids

BoxMG is a geometrically inspired algebraic technique<sup>8, 9, 29</sup> to determine inter-grid transfer operators. In a spacetree context, each fine grid is split up along the next coarser level’s grid lines. We assume that the prolongation from a coarse vertex maps onto the nullspace of the fine grid operator. However, BoxMG does not examine the “real” operator. Instead, it studies an operator which is collapsed along the coarse grid level boundaries.

All fine grid points are classified into  $c$ -points (coinciding spatially with coarse grid points of the next coarser level),  $\gamma$ -points which coincide with the faces of the next coarser levels and  $f$ -points. Prolongation and restriction are the identity on  $c$ -points.

Along  $\gamma$ -points, we collapse the stencil: If  $\gamma$  members reside on a face with normal  $n$ , the stencil is accumulated (lumped) along the  $n$  direction. The result contains only entries along the non- $n$  directions. Higher dimensional collapsing can be constructed iteratively. We solve  $\tilde{A}Pe = 0|_\gamma$ — $\tilde{A}$  stems from the collapsed operators—along these  $\gamma$ -points where  $e$  is the characteristic vertex vector on the coarse grid, i.e. holds one entry 1 and zeroes everywhere else. Finally, we solve  $APe = 0|_f$  for the remaining points. No two  $f$ -points separated by a coarse grid line are coupled to each other anymore.

In<sup>5</sup>, we detail how to store BoxMG’s operators as well as all Rith-Galerkin operators which typically supplement BoxMG within the spacetree. This yields a hybrid scheme in two ways: BoxMG itself is a geometrically inspired way to construct algebraic inter-grid transfer operators. Storing the entries within the spacetree allows for a “matrix-free” implementation with explicit matrix storage.

### 3 | ADDITIVELY DAMPED AFAC SOLVERS WITH FAS AND HTMG

With our ingredients and observations at hand, our research agenda reads as follows: We first introduce our additive multigrid scheme which avoids oscillations without compromising on the convergence speed. Secondly, we discuss two operators suited to realise our scheme. Finally, we contextualise this idea and show that the new solver actually belongs into the family of AFAC solvers.

#### 3.1 | An additively damped additive multigrid solver

Both additive and multiplicative multigrid sum up all the levels’ corrections. Multiplicative multigrid is more stable than additive—it does not overshoot—as each level eliminates error modes tied to its resolution. In practice, we cannot totally separate error modes, and we cannot assume that a correction on level  $\ell$  does not introduce a new error on level  $\ell + 1$ . Multigrid solvers thus often use postsmoothing. Once we ignore this multiplicative lesson learned, the simplest class of multiplicative solvers is  $V(\mu_{pre} = 1, 0)$ .

We start with our recast of the multiplicative  $V(1, 0)$  two-grid cycle (3) into an additive formulation (2). Our objective is to quantify additive multigrid’s “too much” of a correction relative to its multiplicative cousin. For this, we compare the multiplicative two-grid scheme (3) to the two level additive scheme with an exact solve on the coarse level

$$u_{\ell_{max}, add}^{(n+1)} = PA_{\ell_{max}-1}^{-1} R(b_{\ell_{max}} - A_{\ell_{max}} u_{\ell_{max}}^{(n)}) + \left[ u_{\ell_{max}}^{(n)} + \omega_{\ell_{max}} M_{\ell_{max}}^{-1} (b_{\ell_{max}} - A_{\ell_{max}} u_{\ell_{max}}^{(n)}) \right].$$

The difference is

$$\begin{aligned} u_{\ell_{max}, mult}^{(n+1)} - u_{\ell_{max}, add}^{(n+1)} &= PA_{\ell_{max}-1}^{-1} R(b_{\ell_{max}} - A_{\ell_{max}} \left[ u_{\ell_{max}}^{(n)} + \omega_{\ell_{max}} M_{\ell_{max}}^{-1} (b_{\ell_{max}} - A_{\ell_{max}} u_{\ell_{max}}^{(n)}) \right]) \\ &\quad - PA_{\ell_{max}-1}^{-1} R(b_{\ell_{max}} - A_{\ell_{max}} u_{\ell_{max}}^{(n)}). \end{aligned} \quad (5)$$

The superscripts  $^{(n)}$  and  $^{(n+1)}$  denote old respective new iterates of a vector. We continue to omit it from here where possible.

Starting from the additive rewrite of the  $V(1, 0)$  multiplicative two-level scheme, we intend to express multiplicative multigrid as an additive scheme. This is a popular endeavour as additive multigrid tends to scale better. There is no close-to-serial coarse grid solve. There is no coarse grid bottleneck in an Amdahl sense. Multiplicative multigrid however tends to converge faster and is more robust. Different to popular approaches such as Mult-additive<sup>10, 19</sup>, our approach gives up on the idea to achieve the convergence rate of multiplicative multigrid. Instead, we save “solely” the robustness over into the additive regime. Our hypothesis is that any gain in concurrency will eventually outperform efficiency improvements on future machines. A few ideas guide our agenda:

**Idea 1.** We add an additional one-level term to our additive scheme which imitates multiplicative multigrid.

This idea circumscribes (5) where we already stick to a two-grid formalism. Our strategy next is to find an approximation to

$$-PA_{\ell_{max}-1}^{-1} RA_{\ell_{max}} \omega_{\ell_{max}} M_{\ell_{max}}^{-1} (b_{\ell_{max}} - A_{\ell_{max}} u_{\ell_{max}}) \quad (6)$$

from (5) such that we obtain a modified additive two-grid scheme which, on the one hand, mimicks multiplicative stability and, on the other hand, is cheap. For this, we read the difference term as an auxiliary solve.

**Idea 2.** We approximate the auxiliary term (6) with a single smoothing step.

The approach yields a per-level correction

$$-P\omega_{\ell-1}\tilde{M}_{\ell_{\max}-1}^{-1}RA_{\ell_{\max}}\omega_{\ell_{\max}}M_{\ell_{\max}}^{-1}(b_{\ell_{\max}}-A_{\ell_{\max}}u_{\ell_{\max}}). \quad (7)$$

We use the tilde to denote the auxiliary solves. Following Idea 1, this is a per-level correction: When we re-generalise the scheme from two grids to multigrid (by a recursive expansion of  $A_{\ell_{\max}-1}^{-1}$  within the original additive formulation), we do not further expand the correction (6) or (7). This implies another error which we accept in return for a simplistic correction term without additional synchronisation or data flow between levels.

**Idea 3.** The damping runs asynchronously to the actual solve. It is another additive term computed concurrently to each correction equation.

Using  $A_{\ell_{\max}}\omega_{\ell_{\max}}M_{\ell_{\max}}^{-1}$  adds a sequential ingredient to the damping term. A fine grid solve must be finished before it can enter the auxiliary equation. This reduces concurrency. Therefore, we propose to merge this preamble smoothing step into the restriction. This is similar to smoothed aggregation which typically uses a simple aggregation/restriction operator and then improves it by applying a smoother. It is also similar to Mult-additive<sup>19</sup>, which constructs inter-grid transfer operators that pick up multiplicative pre- or post-smoothing behaviour. We apply the smoothed operator concept to the restriction  $\tilde{R} = \omega RAM^{-1}$ , and end up with a wholly additive correction term

$$-\tilde{\omega}P\tilde{M}_{\ell_{\max}-1}^{-1}\tilde{R}. \quad (8)$$

**Idea 4.** We identify the auxiliary coarse grid levels with the actual multilevel grid hierarchy. All resolution levels integrate into the spacetime.

$\tilde{M}$  and  $\tilde{A}$  are auxiliary operators but act on mesh levels which we hold anyway. With the spacetime at hand, we finally unfold the two-grid scheme into

$$\begin{aligned} u_{\ell_{\max}} \leftarrow u_{\ell_{\max}} &+ \left( \sum_{\ell=\ell_{\min}}^{\ell_{\max}} \omega_{add}(\ell) P^{\ell_{\max}-\ell} M_{\ell}^{-1} R^{\ell_{\max}-\ell} \right) (b_{\ell_{\max}} - A_{\ell_{\max}} u_{\ell_{\max}}) \\ &- \left( \sum_{\ell=\ell_{\min}}^{\ell_{\max}} \tilde{\omega}_{add}(\ell) P^{\ell_{\max}-\ell} \tilde{M}_{\ell}^{-1} \tilde{R}^{\ell_{\max}-\ell} \right) (b_{\ell_{\max}} - A_{\ell_{\max}} u_{\ell_{\max}}), \end{aligned} \quad (9)$$

where we set, without loss of generality,  $M_{\ell_{\max}-1}^{-1} = 0$ . This assumes that no level coarser than  $\ell_{\min}$  hosts any degree of freedom.

---

**Algorithm 1** Blueprint of one sweep of the our adAFAC-Jac.  $R^i$  or  $P^i$  denote the recursive application of the restriction or prolongation, respectively.  $\tilde{R}^i$  is the repeated application of  $R^j$  up to  $j = i - 1$  followed by an application of one smoothed operators.

---

**function** ADAFACX

$r_{\ell_{\max}} \leftarrow b_{\ell_{\max}} - A_{\ell_{\max}} u_{\ell_{\max}}$

**for all**  $\ell_{\min} \leq \ell < \ell_{\max}$  **do**

$b_{\ell} \leftarrow R^{\ell_{\max}-\ell} r_{\ell_{\max}}$

▷ Restrict fine grid residual to grid level  $\ell$

**end for**

**for all**  $\ell_{\min} \leq \ell < \ell_{\max}$  **do**

$\tilde{b}_{\ell} \leftarrow \tilde{R}^{\ell_{\max}-\ell} r_{\ell_{\max}}$

▷ Additional restriction residual into additional grid space

**end for**

**for all**  $\ell_{\min} \leq \ell < \ell_{\max}$  **do**

$c_{\ell} \leftarrow 0; \tilde{c}_{\ell} \leftarrow 0$

JACOBI( $A_{\ell} c_{\ell} = b_{\ell}, \omega$ )

▷ Iterate of correction equation stored in  $c_{\ell}$

JACOBI( $\tilde{A}_{\ell} \tilde{c}_{\ell} = \tilde{b}_{\ell}, \tilde{\omega}$ )

▷ Iterate of correction equation stored in  $\tilde{c}_{\ell}$

**end for**

$c_{\ell_{\max}} \leftarrow 0$

JACOBI( $A_{\ell_{\max}} c_{\ell_{\max}} = b_{\ell_{\max}}, \omega$ )

$u_{\ell_{\max}} \leftarrow u_{\ell_{\max}} + c_{\ell_{\max}} + \sum_{\ell=\ell_{\min}}^{\ell_{\max}-1} P^{\ell_{\max}-\ell} c_{\ell} - P^{\ell_{\max}-\ell} \tilde{c}_{\ell}$

**end function**

---

### 3.2 | Two damping operator choices

It is obvious that the effectiveness of the approach depends on a proper construction of (8). We propose two variants. Both accept that smoothed inter-grid transfer operators yield better operators than standard bi- and trilinear operators (and obviously naive injection or piecewise constant interpolation)<sup>16–18</sup>. Simple geometric transfer operators fail to capture complex solution behaviour<sup>30–32</sup> for non-trivial  $\epsilon$  choices in (1).

Let  $\epsilon$  in (1) be one. We observe that a smoothed operator derived from bilinear interpolation for three-partitioning equals

$$\begin{bmatrix} -0.0139 & -0.0417 & -0.0833 & -0.0972 & -0.083 & -0.0417 & -0.0139 \\ -0.0417 & 0 & 0 & 0.0833 & 0 & 0 & -0.0417 \\ -0.0833 & 0 & 0 & 0.167 & 0 & 0 & -0.0833 \\ -0.0972 & 0.0833 & 0.167 & 0.44444444 & 0.167 & 0.0833 & -0.0972 \\ -0.0833 & 0 & 0 & 0.167 & 0 & 0 & -0.0833 \\ -0.0417 & 0 & 0 & 0.0833 & 0 & 0 & -0.0417 \\ -0.0139 & -0.0417 & -0.0833 & -0.0972 & -0.0833 & -0.0417 & -0.0139 \end{bmatrix}.$$

Assuming  $\epsilon = 1$  is reasonable as the term  $A_\ell M_\ell^{-1}$  or  $M_{\ell-1}^{-1} R A_\ell$ , respectively, enters the auxiliary restriction. Such an expression removes the impact of  $\epsilon$ —it yields the Laplacian—on all elements with non-variable  $\epsilon$ . Assuming  $\epsilon$  is reasonably smooth, we neglect only small perturbations in the off-diagonals of the system matrix.

---

**Algorithm 2** Blueprint of our adAFAC-PI.  $R^i$  or  $P^i$  denote the recursive application of the single level restriction or prolongation,  $R$  or  $P$ , respectively.  $I$  is the injection operator.

---

**function** ADAFACX

$r_{\ell_{\max}} \leftarrow b_{\ell_{\max}} - A_{\ell_{\max}} u_{\ell_{\max}}$

**for all**  $\ell_{\min} \leq \ell \leq \ell_{\max}$  **do**

$b_\ell \leftarrow R^{\ell_{\max}-\ell} r_{\ell_{\max}}$

▷ Restrict fine grid residual to grid level  $\ell$

**end for**

**for all**  $\ell_{\min} < \ell \leq \ell_{\max}$  **do**

$c_\ell \leftarrow 0; \tilde{c}_\ell \leftarrow 0$

JACOBI( $A_\ell c_\ell = b_\ell, \omega$ )

▷ Iterate of correction equation stored in  $c_\ell$

$\tilde{c}_\ell \leftarrow P I c_\ell$

▷ Computation of localised damping for  $c_\ell$

**end for**

$c_{\ell_{\min}} \leftarrow 0$

JACOBI( $A_{\ell_{\min}} c_{\ell_{\min}} = b_{\ell_{\min}}, \omega$ )

$u_{\ell_{\max}} \leftarrow u_{\ell_{\max}} + c_{\ell_{\min}} + \sum_{\ell=\ell_{\max}}^{\ell_{\min}-1} P^{\ell_{\max}-\ell} c_\ell - P^{\ell_{\max}-\ell} \tilde{c}_\ell$

**end function**

---

This motivates us introduce two modified, i.e. smoothed restriction operators  $\tilde{R}$ :

1. A “smoothed”  $\tilde{R} = \omega R A M_\ell^{-1}$ . Implementations may truncate the support, i.e. throw away the smallish negative entries by which the stencil support grows, and approximate  $\tilde{M}_{\ell-1} = M_{\ell-1}$ . For this choice, memory requirements are slightly increased (we have to track one more “unknown”) and two solves on all grid level besides on the finest mesh are required (Algorithm 1).
2. Sole injection which can be seen as a mass-lumped smoothed stencil. In this case, we collapse  $\tilde{M}_{\ell-1} I A_\ell$  into the identity. The overall damping reduces to  $-\omega P I M_\ell^{-1}$ . We evaluate the original additive solution update. While we perform this update, we identify updates within  $c$ -points, i.e. for vertices spatially coinciding with the next coarser mesh, inject these, immediately prolongate them down again, and damp the overall solution with the result. The damping equation is  $P I$  (Algorithm 2).

Both choices are motivated through empirical observations. Our results study them for jumping coefficients in complicated domains, while our previous work demonstrates the suitability for Helmholtz-type setups<sup>4</sup>. Though the outcome of both approaches is promising for our tests, we hypothesise that more complicated setups such as convection-dominated phenomena require more care in the choice of  $\tilde{R}$ , as  $R$  has to be chosen more carefully<sup>29</sup>.



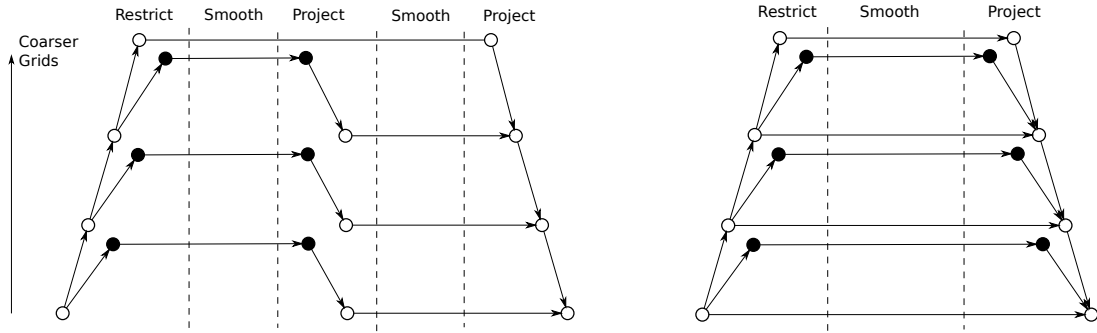


**FIGURE 2** Schematic overview of AFACx (left) and our adAFAC (right). Black markers denote smoothing steps on the auxiliary equations, white markers correspond to traditional additive multigrid.

Both approaches can be combined with multigrid with geometric transfer operators where  $P$  is  $d$ -linear everywhere or with algebraic approaches where  $P$  stems from BoxMG. Both approaches inherit Ritz-Galerkin operators if they are used in the baseline additive scheme. Otherwise, they exploit rediscretisation.

### 3.3 | The AFAC solver family and further related approaches

It is not a new idea to damp FAC's additive formulation such that additive multigrid remains stable. Among the earliest endeavours is FAC's asynchronous variant AFAC<sup>13, 14</sup> which decouples the individual grid levels to yield higher concurrency, too. To remove oscillations, AFAC is traditionally served in two variants<sup>22</sup>:

AFACc simultaneously determines the right-hand side for all grid levels  $\ell$ . Before it restricts the fine grid residual to a particular level  $\ell$ , any residuals on vertices spatially coinciding with vertices on the level  $\ell$  are set to zero. They are masked out. This effectively damps the correction equation's right-hand side. If we applied this residual masking recursively—a discussion explicitly not found in the original AFACc paper where only the points are masked which coincide with the target grid—i.e. if we constructed the masking restriction recursively over the levels instead of in one rush, then AFACc would become a hybrid solver between additive multigrid and the hierarchical basis approach<sup>22</sup>.

AFACf goes down a different route: The individual levels are treated independently from each other, but each level's right-hand side is damped by an additional coarse grid contribution. This coarse grid contribution is an approximate solve of the correction term for the particular grid. AFACf solves all meshes in parallel and sums up their contributions, but each mesh has reduced its contribution by its local additional coarse grid cycle. The resulting scheme is similar to the combination technique as introduced for sparse grids<sup>33</sup>: We determine all solution updates additively but remove the intersection of their coarser meshes.

Since multiplicative methods are superior to additive in terms of stability and simplicity, the transition from AFAC into AFACx<sup>14</sup> is seminal: Its inventors retain one auxiliary coarser level for each multigrid level, and split the additive scheme's solve into two phases (Figure 2): A first phase determines per level which modi might be eliminated by coarser grid solves. For this, they employ the auxiliary helper level. Each level keeps its additive right-hand side in the second phase, but it starts with a projection from this auxiliary level as an initial guess. The projection damps the correction after smoothing. Only the resultant damped corrections derived in the second phase are eventually propagated to finer grids.

AFAC and FAC solvers traditionally remain vague which solvers are to be used for particular substeps. They are meta algorithms and describe a family of solvers. AFACx publications allow a free, independent choice of multigrid hierarchy and auxiliary levels. Our approach is different. We stick to the spacetime construction paradigm. As a result, real and auxiliary grid levels coincide. Furthermore, we do not follow AFACx's multiplicative per-level update (anticipate first the corrections made on coarser grids and then determine own grid's contribution). Instead, we run two computations in parallel (additively). One is the classic additive correction computation. The other term imitates the reduction of this update as compared to multiplicative multigrid. This additional, auxiliary term is subject to a single smoothing step on one single auxiliary level which is the same as the next additive resolution.

Our approach shares ideas with the Mult-additive approach<sup>19</sup> where smoothed transfer operators are used to approximate a  $V(1, 1)$  cycle. Mult-additive yields faster convergence as it effectively yields stronger smoothers. We stick to the simple pre-smoothing approach and solely hijack the additional term to circumvent overshooting, while the asynchrony of the individual levels is preserved.

We finally observe that our solver variant with a  $PI$ -term exhibits some similarity with BPX. BPX builds up its correction solely through inter-grid transfer operators while the actual fine grid system matrix does not directly enter the correction equations. Though not delivering an explanation why the solver converges, the introduction of the  $PI$ -scheme in<sup>4</sup> thus refers to this solver as BPX-like.

**Idea 5.** As our solver variants are close to AFAC, we call them adaptively damped AFAC and use the postfix  $PI$  or  $Jac$  to identify which damping equations we employ. Our manuscript thus introduces adAFAC-PI and adAFAC-Jac.

## 4 | AN ELEMENT-WISE, SINGLE-TOUCH IMPLEMENTATION

---

**Algorithm 3** Outline of single-touch adAFAC-Jac. adAFAC-PI is presented in<sup>4</sup>.  $sc$  is the summed coarse grid correction contributions.  $sf$  is the summed fine grid correction contributions.  $sl$  is the summed local grid correction contributions. A tilde identifies variables related to the auxiliary adAFAC grid. We invoke the cycle passing in the coarsest grid  $\ell_{min}$ .

---

```

function ADAFACX( $\ell$ )
   $u_\ell \leftarrow u_\ell + P_{\ell-1}^\ell sc_{\ell-1} - \tilde{sl}$                                 ▷ Prolong contributions from both grids
   $u_\ell \leftarrow u_\ell + sf_\ell - \tilde{sf}_\ell$                                 ▷ Anticipate fine grid smoothing effects
   $sc_\ell \leftarrow sl_\ell - \tilde{sl}_\ell + P_{\ell-1}^\ell sc_{\ell-1} - P_{\ell-1}^\ell \tilde{sl}_{\ell-1}$     ▷ Prepare for further prolongation
   $\hat{u}_\ell \leftarrow u_\ell - P_{\ell-1}^\ell Iu_{\ell-1}$                                 ▷ Determine hierarchical residual
   $b_\ell \leftarrow 0; \tilde{b}_\ell \leftarrow 0$                                 ▷ Reset RHS of correction equations
  if  $\ell \neq \ell_{max}$  then
    ADAFACX( $\ell + 1$ )
  end if
   $d_\ell = \text{JACOBI}(A_\ell u_\ell = b_\ell, \omega)$                                 ▷ Determine update through Jacobi step
   $\tilde{d}_\ell = \text{JACOBI}(\tilde{A}_\ell \tilde{u}_\ell = \tilde{b}_\ell, \omega)$ 
   $r_\ell \leftarrow \text{RESIDUAL}(A_\ell u_\ell = b_\ell)$                                 ▷ Bookmark residual from Jacobi update
   $\hat{r}_\ell \leftarrow \text{RESIDUAL}(\tilde{A}_\ell \tilde{u}_\ell = \tilde{b}_\ell)$                                 ▷ Compute hierarchical residual
   $sl_\ell \leftarrow d_\ell; u_\ell \leftarrow u_\ell + d_\ell; \tilde{sl}_\ell \leftarrow \tilde{d}_\ell$     ▷ Bookmark and apply updates
   $b_\ell \leftarrow R_{\ell-1}^{\ell-1} \hat{r}_{\ell+1}; \tilde{b}_\ell \leftarrow \tilde{R}_{\ell-1}^{\ell-1} \hat{r}_{\ell+1}$     ▷ Restrict RHS to coarse equation systems
   $sf_{\ell-1} \leftarrow I(sf_\ell + sl_\ell)$                                 ▷ Inform all levels about updates
   $\tilde{sf}_{\ell-1} \leftarrow I(\tilde{sf}_\ell + \tilde{sl}_\ell)$                                 ▷ Do not apply them
end function

```

---

adAFAC fits seamlessly to our algorithmic building blocks. It solves up to three equations of the same type per level. Lets distinguish the unknowns of these equations as follows:  $u$  is the solution in a FAS multiscale sense, while  $\hat{u}$  is the hierarchical solution required for HTMG. We do not need an additional  $\tilde{u}$  adAFAC unknown. adAFAC solves a correction equation, but no solution equation in the FAS sense. A complicated multi-scale representation along resolution boundaries is thus not required for the auxiliary damping equation: No semantic distinction between solution and correction areas is required. Let  $d$  and  $\tilde{d}$  encode the iterative updates of the unknowns through the additive FAS scheme or the auxiliary adAFAC equation, respectively.

### 4.1 | Operator storage

To make adAFAC stable and efficient for non-trivial  $\epsilon$ , each vertex stores its operator parts from  $A$ . Vertices hold the stencils. For vertex members of the finest grid, the stiffness matrix entries result from the discretisation of (1). If we use  $d$ -linear inter-grid

transfer operators this storage scheme is applied to all levels. Otherwise, we augment each vertex by further stencils for  $P$  and  $R$  and proceed as follows: For a vertex on a particular level which overlaps with finer resolutions, this vertex belongs to a correction equation. Its stencil results from the Ritz-Galerkin coarse grid operator definition, whereas the inter-grid transfer operators  $P$  and  $R$  result from Dendy's BoxMG<sup>8</sup>. BoxMG is well-suited for three-partitioning<sup>5, 9, 29</sup>. We refer to<sup>5</sup> for remarks how to make the scheme effectively matrix-free, i.e. memory saving, nevertheless. Each coarse grid vertex carries its prolongation and restriction operator plus its stencil. We are also required to store the auxiliary  $\tilde{R}$  for adAFAC-Jac. All further adAFAC terms use operators already held.

## 4.2 | Grid traversal

For the realisation of the (dynamically) adaptive scheme, we follow<sup>3-5, 34</sup> and propose to run through the spacetree in a depth-first (DFS) manner while each level's cells are organised along a space-filling curve (SFC)<sup>2</sup>. We write the code as recursive function where each cell has access to its  $2^d$  adjacent vertices, its parent cell, and the parent cell's  $2^d$  adjacent vertices. The latter ingredients are implicitly stored on the call stack of the recursive function.

As we combine DFS with space-filling curves, our tree traversal is weakly single-touch w.r.t. the vertices: Vertices are loaded when an adjacent cell from the spacetree is first entered. They are "touched" for the last time when the  $2^d$ th adjacent cell within the spacetree is left due to recursion backtracking. In-between, they reside either on the call stack or can be temporarily stored in stacks<sup>2</sup>. The call stack is bounded by the depth of the spacetree—it is small—while all temporary stacks are bounded by the time in-between the traversal of two face-connected cells. The latter is short due to the Hölder continuity of the underlying SFC. Hanging vertices per grid level, i.e. vertices surrounded by less than  $2^d$  cells, are created on-demand on-the-fly. They are not held persistently. We may assume that all data remains in the caches<sup>2, 3, 34</sup>.

As we extract element-wise operators for  $A, P, R$  from the stencils stored within the vertices or hard-code these element-wise operators, we end up with a strict element-wise traversal in a multiscale sense. All matrix-vector products (mat-vecs) are accumulated. The realisation of the element-wise mat-vecs reads as follows: Once we have loaded the vertices adjacent to a cell, we can derive the element-wise stiffness matrix or inter-grid transfer operator for the cell. To evaluate  $r = Au$ , we set one variable  $r$  per vertex to zero, and then accumulate the matrix-vector (mat-vec) contributions in each of the vertex's adjacent cells. Since the hierarchical  $\hat{u}$  can be determined on-the-fly while running DFS from coarse grids into fine grids, the evaluation of  $\hat{r}$  follows exactly  $r$ 's pattern. So does the realisation of  $\tilde{r}$ . adAFAC's mat-vecs can be realised within a single spacetree traversal. The mat-vecs are single-touch.

## 4.3 | Logical iterate shifts and pipelining

A FAS sweep however can not straightforwardly be realised within a single DFS grid sweep<sup>4</sup>: The residual computation propagates information bottom-up, the corrections propagate information top-down, and the final FAS injection propagates information bottom-up again. This yields a cycle of causal dependencies. We thus offset the additive cycle's smoothing steps by half a grid sweep: Each grid sweep, i.e. DFS traversal, evaluates all three mat-vecs—of FAS, of HTMG, of adAFAC—but does not perform the actual updates. Instead, correction quantities  $sl, sc, sf, \tilde{sc}, \tilde{sf}$ , and  $\tilde{sl}$  are bookmarked as additional attributes within the vertices while the grid traversal backtracks, i.e. returns from the fine grids to the coarser ones. Their impact is added to the solution throughout the downstepping of the subsequent tree sweep. Here, we also evaluate the prolongation. Restriction of the residual to the auxiliary right-hand side and hierarchical residual continue to be the last action on the vertices at the end of the sweep when variables are last written/accessed. As we plug into the recursive function's backtracking, we know that all right-hand sides are accumulated from finer grid levels when we touch a vertex for the last time throughout a multiscale grid traversal. We can thus compute the unknown updates though we do not directly apply them.

As we use helper variables to store intermediate results throughout the solve and apply them the next time, we need one tree traversal per V-cycle plus one kick-off traversal. Our helper variables pick up ideas behind pipelining and are a direct translation of optimisation techniques proposed in<sup>4</sup> to our scheme. Per traversal, each unknown is read into memory/caches only once. We obtain a single-touch implementation. adAFAC's auxiliary equations do not harm its suitedness to architectures with a widening memory-compute facilities gap.

Dynamic mesh refinement integrates seamlessly into the single-touch traversal: We rely on a top-down tree traversal which adds additional tree levels on-demand throughout the steps down in the grid hierarchy. The top-down traversal's backtracking drops parts of the tree if a coarsening criterion demands so. It erases mesh parts. Though erasing feature is not required

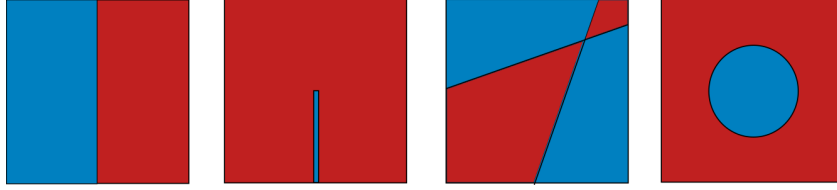


**FIGURE 3** The four  $\epsilon$  distributions studies throughout the tests. The blue area (left; inside of the inclusion; top left and bottom right; or inside the circle respectively) holds  $\epsilon = 1$ . The remaining domain  $\epsilon = 10^{-k}$ ,  $k \in \{1, 2, \dots, 5\}$ .

for the present test cases, both refinement and coarsening integrate into Algorithm 3. We inherit FAC's straightforward handling of dynamic adaptivity, simply the treatment of resolution transitions through FAS, and provide an implementation which reads/writes each unknown only once from the main memory.

## 5 | NUMERICAL RESULTS

To assess the potential of adAFAC, we study three test setups of type (1) on the unit square. They are simplistic yet already challenging for multigrid. All setups use  $f = 0$  and set  $u|_{\partial\Omega} = 1$  for  $x_2 = 0$  and  $u|_{\partial\Omega} = 0$  otherwise. A first test is the sole Poisson equation with a homogeneous material parameter. The three other setups (Figure 3) use regions with  $\epsilon = 1$  and regions with  $\epsilon = 10^{-k}$ . Per run, the respective  $k \in \{1, 2, \dots, 5\}$  is fixed. The second setup splits up the parameter domain into two equally sized sections. We emphasise that the split is axis-aligned but does not coincide with the mesh as we employ three-partitioning of the unit square. The third setup penetrates the area with a thin protruding line of width 0.02. This line is parameterised with  $\epsilon$ . It extends from the  $x_0$  axis— $(x_1, x_2)^T \in \mathbb{R}^2$  are the coordinate axes—and terminates half-way into the domain. Such small material inhomogeneities cannot be represented explicitly on coarse meshes. The last setup makes the lines  $x_2 = 5x_1 - 2.5$  and  $x_2 = 0.2x_1 + 0.5$  separate domains which hold different  $\epsilon$  in a checkerboard fashion. No parameter split is axis-aligned.

Our experiments always focus on  $d = 2$  and start with a 2-grid algorithm ( $\ell_{\max} = 2$ ) where the coarser level has  $(3 - 1)^d = 4$  degrees of freedom and the finer level hosts  $(3^2 - 1)^d = 64$  vertices carrying degrees of freedom. From hereon, we add further grid levels and build up to a 7- or 8-grid scheme ( $\ell_{\max} = 7$  or  $\ell_{\max} = 8$ ). The parameter  $\ell_{\max}$  uniquely defines the experiment. For two different  $\ell_{\max}$  values, the meshes differ in number of grid levels, and they also differ in degree of freedom counts.

If tests are labelled as regular grid runs, each grid level is regular and we consequently end up with a mesh holding  $(3^7 - 1)^d = 4,778,596$  degrees of freedom for  $\ell_{\max} = 7$ . If not labelled as regular grid run, our tests rely on dynamic mesh refinement. We start from the regular grid of depth  $\ell = 2$ . In every other cycle, our code manually refines the cells along the bottom boundary, i.e. the cells where one face carries  $u|_{\partial\Omega} \neq 0$ . We stop with this refinement when the grid meets  $\ell_{\max}$ . Our manual mesh construction ensures that we kick off with a low total vertex count, while the solver does not suffer from pollution effects: The scheme kickstarts further feature-based refinement. Parallel to the manual refinement along the boundary, our implementation measures the absolute second derivatives of the solution along both coordinate axes in every single unknown. A bin sorting algorithm is used to identify the vertices carrying the (approximately) 10 percent biggest directional derivatives. These are refined unless they already meet  $\ell_{\max}$ . The overall approach is similar to full multigrid where coarse grid solutions serve as initial guesses for subsequent cycles on finer meshes, though our implementation lacks higher-order operators. All interpolation from coarse to fine meshes both for hanging vertices and for newly created vertices is  $d$ -linear.

Our runs employ a damped Jacobi smoother with damping  $\omega = 0.6$  and report the normalised residuals

$$\frac{\|r^{(n)}\|_h}{\|r^{(0)}\|_h} \quad \text{where} \quad \|r^{(n)}\|_h := \sum_i h_i^d (r_i^{(n)})^2, \quad (10)$$

with  $n$  being the cycle count.  $r_i^{(n)}$  is the residual in vertex  $i$  and  $h_i$  is the local mesh spacing around vertex  $i$ . Dynamic mesh refinement inserts additional vertices and thus might increase the residual vectors between two subsequent iterations. As a consequence, residuals under an Eulerian norm may temporarily grow due to mesh expansion. This effect is amplified by the lack of higher order interpolation for new vertices. The normalised residual (10) enables us to quantify how much the residual has decreased compared to the residual fed into the very first cycle.

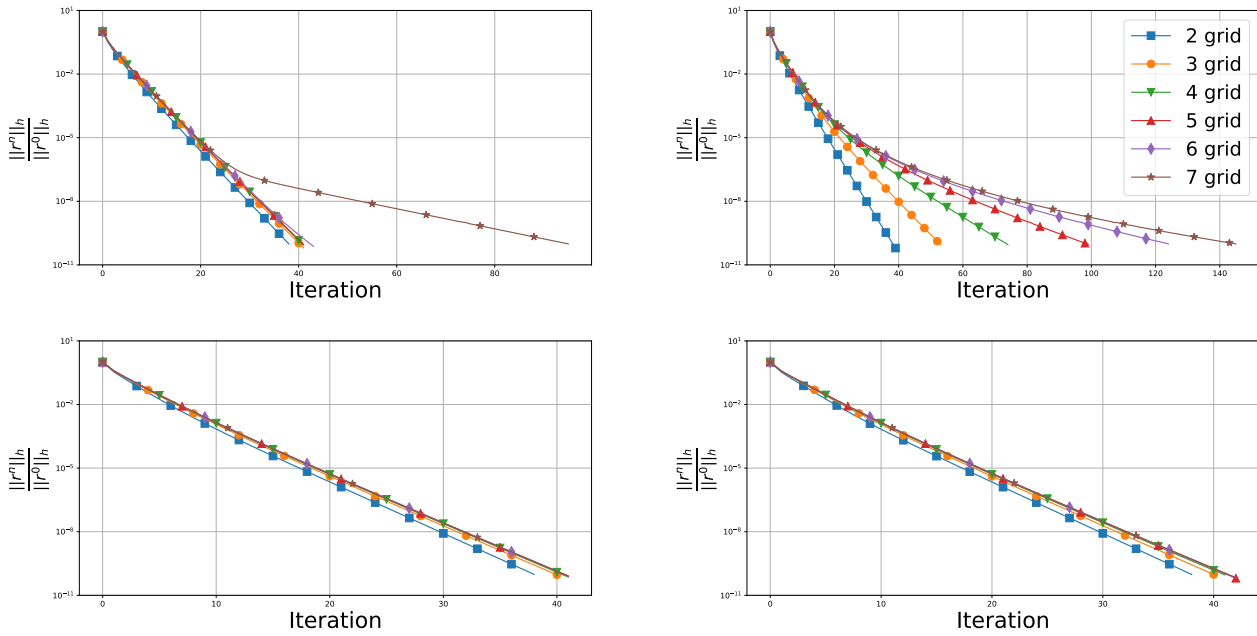


**FIGURE 4** Solves of the Poisson equation on regular grids of different levels. We compare plain additive multigrid (top, left), multigrid using exponential damping (top, right), adAFAC-PI (bottom, left) and adAFAC-Jac (bottom, right).

Where appropriate, we also display the normalised maximum residual

$$\frac{\max_i \{|r_i^{(n)}|\}}{\max_i \{|r_i^{(0)}|\}}.$$

This metric identifies localised errors, while (10) weights errors with the mesh size.

## 5.1 | Consistency study: the Poisson equation

Our first set of experiments focuses on the Poisson equation, i.e.  $\epsilon = 1$  everywhere. Multigrid is expected to yield a perfect solver for this setup: Each cycle (multiscale grid sweep) has to reduce the residual by a constant factor which is independent of the degrees of freedom, i.e. number of vertices. Ritz-Galerkin multigrid yields the same operators as rediscretisation, since BoxMG gives bilinear inter-grid transfer operators. The setup is a natural choice to validate the consistency and correctness of the adaFACx ingredients. All grids are regular.

Our experiments (Figure 4) confirm that additive multigrid is insignificantly faster than the other alternatives if it is stable. The more grid levels are added, the more we overshoot per multilevel relaxation. When we start to add a seventh level, this suddenly makes the plain additive code’s performance deteriorate. With an eighth level added, the solver would diverge (not shown). Exponentially damped multigrid does not suffer from the instability for lots of levels, but its damping of coarse grid influence leads to the situation that long-range solution updates don’t propagate quickly. The convergence speed suffers from additional degrees of freedom. Both of our adAFAC variants are stable, but they do not suffer from a speed deterioration. Their “clever”, localised damping pays off. We play in the same league additive multigrid in terms of speed. adAFAC-PI and adAFAC-Jac are almost indistinguishable.

Despite the instability of plain additive multigrid, we continue to benchmark against the undamped additive scheme, as exponential damping is not competitive. All experiments from hereon are reasonable irregular/coarse to circumnavigate the instabilities. Feature-based dynamic refinement criterion makes the mesh spread out from the bottom edge where  $u|_{\partial\Omega} = 1$  (Figure 5). To assess its impact on cost, we count the number of required degrees of freedom updates plus the updates on coarser levels. We do not neglect the coarse grid costs.

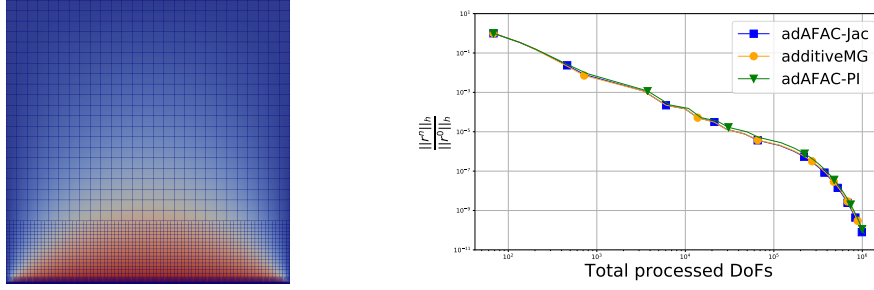


**FIGURE 5** Left: Typical adaptive mesh for pure Poisson (constant material parameter) once the refinement criterion has stopped adding further elements. Right: We compare different solvers on the pure Poisson equation using a hybrid FMG-AMR approach starting at a two grid scheme and stopping at an eight grid scheme.  $\ell_{max} = 8$ .

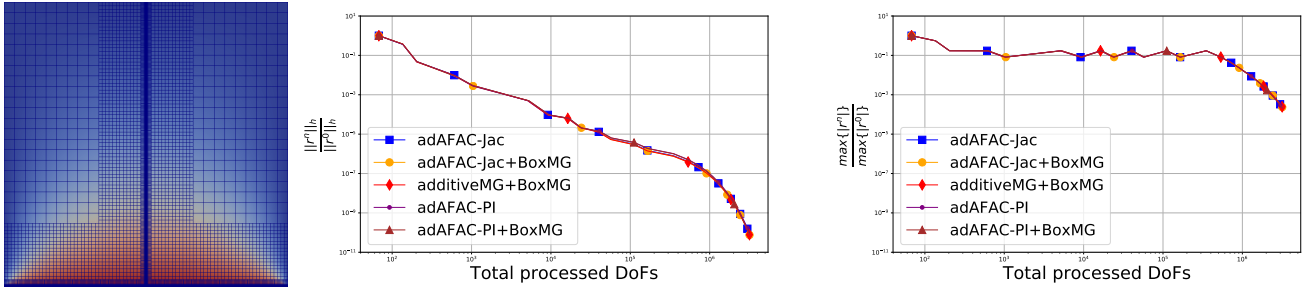


**FIGURE 6** Domain material is split into two halves with an  $\epsilon$  jump from  $\epsilon = 1$  to  $\epsilon = 0.1$ . Typical adaptive mesh for single discontinuity setup once the refinement criterion has stopped adding further elements (left). The centre plot shows the normalised residual and the right shows the normalised  $L^\infty$ -norm of the residual.  $\ell_{max} = 8$ .

One smoothing step on a regular mesh of level eight yields  $4.3 \cdot 10^7$  updates plus the updates on the correction levels. If the solver terminated in 40 cycles, we would have to invest more than  $10^9$  updates. Dynamic mesh unfolding reduces the cost to reduce the residual by up to three orders of magnitude. For Poisson, this saving applies to both our adAFAC variants and plain additive multigrid, while the latter remains stable.

If ran with BoxMG, our code base uses Ritz-Galerkin coarse operator construction for both the correction terms and the auxiliary adAFAC operators in adAFAC-Jac. We validated that both the algebraic inter-grid transfer operators and geometric operators yield exactly the same outcome. This is correct for Poisson as BoxMG yields geometric operators here and Ritz-Galerkin coarse operator construction for the correction terms thus yields the same result as rediscretisation.

*Observation 1.* Our code is consistent. For very simple, homogeneous setups, it however makes only limited sense to use adAFAC—unless there are many grid levels. If adAFAC is to be used, adAFAC-PI is sufficient. There’s no need to really solve an additional auxiliary equation.

## 5.2 | One material jump

We next study a setup where the material “jumps” in the middle of the domain. All experiments use the AMR/FMG setup, i.e. start from a coarse mesh and then dynamically adapt the grid. We observe that the hard-coded grid refinement refines along the stimulus boundary at the bottom, while the dynamic refinement criterion unfolds it along the material transition (Figure 6). The stronger the material transition is the more important it is to pick up the  $\epsilon$  changes in the inter-grid transfer operators. Otherwise, prolongation of coarse grid corrections yields errors close to  $x_1 = 0.5$ . As no grid in the present setup has degrees of freedom exactly on the material transition, the inter-grid transfer operators are never able to mirror the material transition

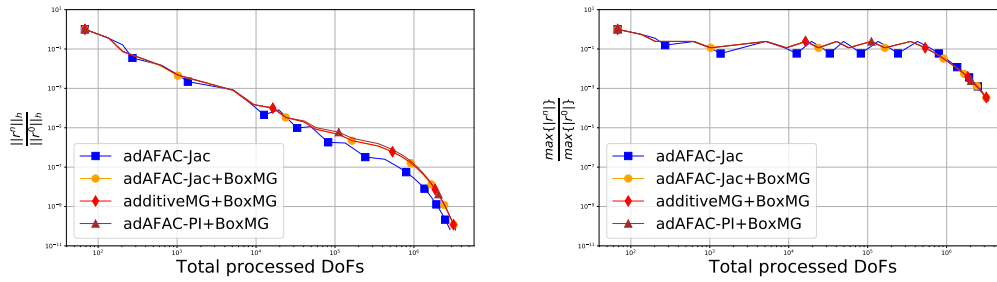


**FIGURE 7** Setup of Figure 6 but with a five orders of magnitude jump in the material parameter. We present only data for converging runs.

exactly. It is the dynamic adaptivity which counterbalances this shortcoming: Large errors in  $P$  are compensated by many corrections on finer grids.

Starting from reasonably small changes in  $\epsilon$  (Figure 6), additive multigrid fails to converge without the addition of BoxMG. Once BoxMG is used, it however becomes stable. This is reasonable, as the residual plot in the maximum norm validates our statement that large errors arise along the material transition when we insert new degrees of freedom. We need an algebraic interpolation routine. Our adAFAC variants in contrast all converge. The absence of a higher-order interpolation for new degrees of freedom hurts, but it does not destroy the overall stability. Once the dynamic AMR stops inserting new vertices—this happens after around  $10^6$  degrees of freedom have been processed—the residual drops under both norms.

The picture changes when we increase the variation in  $\epsilon$ . adAFAC-Jac with bilinear transfer operators converges for all  $\epsilon = 10^{-k}$  values tested, whereas additive multigrid and adAFAC-PI diverge without BoxMG (Figure 7). The geometric inter-grid transfer approach suffers from oscillations around the material transition. All stable solvers play in the same league.

*Observation 2.* If we face reasonably small jumping materials, adAFAC-PI is superior to plain additive multigrid, adAFAC-Jac or any algebraic-geometric extension, as it is both stable and simple to compute. Once the jump grows, adAFAC-Jac becomes the method of choice. Its auxiliary damping equations compensates for the lack of algebraic inter-grid transfer operators which are typically not cheap to compute.

### 5.3 | A material inclusion

Tiny, localised variations in  $\epsilon$  are notoriously difficult to handle for multigrid. The spike setup from our test suite yields a problem where diffusive behaviour is “broken” along the inclusion. The adaptivity criterion thus immediately refines along the tiny material spike (Figure 8) since the solution’s curvature and gradient there is very high. We see diffusive behaviour around this refined area, but we know that there is no long-range, smooth solution component overlapping the  $\epsilon$  changes.

Again, a reasonable small variation in  $\epsilon$  does not pose major difficulties to either of our damped adAFAC solvers. The strong localisation of the adaptivity ensures that the material transition is reasonably handled, such that a sole geometric choice of inter-grid transfer operators is totally sufficient. However, this setup is challenging for additive multigrid which fails to converge even with BoxMG.

Once we increase the material change by three orders of magnitude, we need an explicit elimination of oscillations arising along the  $\epsilon$  changes. Solely employing algebraic BoxMG operators is insufficient. They can mirror the solution behaviour to some degree but they are incapable to compensate for the poor choice of our coarse grid points. The present setup would require algebraic coarse grid identification where the coarse grid aligns with the inclusion.

While adAFAC-PI with algebraic operators manages to obtain reasonable convergence for a material variation of one order of magnitude nevertheless, it is unable to converge for three orders of magnitude change even with algebraic inter-grid transfer operators. adAFAC-Jac is able to handle the sharp, localised transition which also can be read as extreme case of an anisotropic  $\epsilon$  choice in (1). We see convergence for both its geometric variant and its algebraic extension, though now the BoxMG variant is superior to its geometric counterpart.

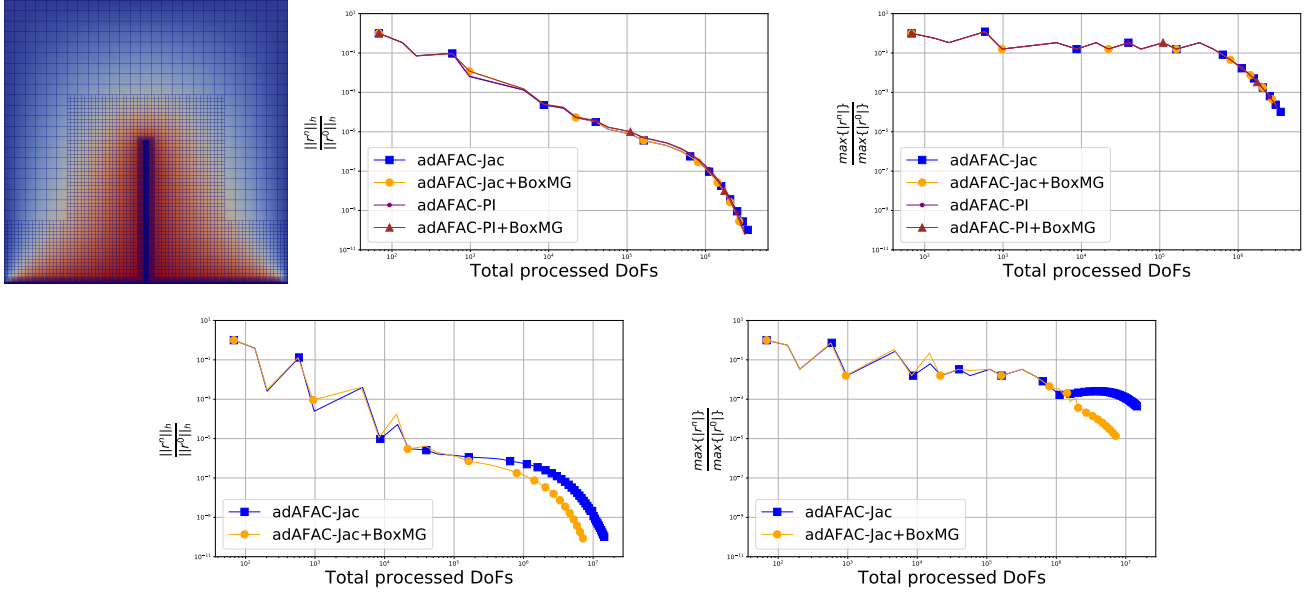


**FIGURE 8** Typical adaptive mesh for setup with a tiny, needle-like inclusion once the refinement criterion has stopped adding further elements (top left). The material inclusion either holds an  $\epsilon$  which is bigger than its surrounding by a factor of ten (top row) or even by a factor of 1,000 (bottom row).

*Observation 3.* adAFAC-Jac equips the geometric-algebraic BoxMG method with the opportunity to compensate, to some degree, for the lack of support of anisotropic refinement.

## 5.4 | Non axis-aligned subdomains

We move on to our experimental setup with a deformed checkerboard setup (Figure 9), where the dynamic adaptivity criterion unfolds the mesh along the material transitions. The solution behaviour within the four subregions itself is smooth, i.e. diffusive, and the adaptivity around the material transitions thus is wider, more balanced, than the hard-coded adaptivity directly at the bottom of the domain.

With smallish variations in  $\epsilon$ , this setup does not pose a challenge to any of our solvers, irrespectible whether they work with algebraic or geometric inter-grid transfer operators. With increasing differences in  $\epsilon$ , we however observe that additive multigrid starts to diverge. The smooth regions are still sufficiently dominant, and we suffer from overcorrection. adAFAC-PI performs better yet requires algebraic operators to remain robust up to  $\epsilon$  variations of three orders of magnitude. adAFAC-Jac with geometric operators remains stable for all studied setups, up to and including the five order of magnitude jump. adAFAC-Jac with algebraic operators outperforms its geometric cousin. BoxMG's accurate handling of material transitions decouples the subdomains from each other on the coarse correction levels. Updates in one domain thus do not pollute the solution in a neighbouring domain.

*Observation 4.* While the auxiliary equations can replace/exchange algebraic operators in some cases, they fail to tackle material transitions that are not grid-aligned.

## 6 | CONCLUSION AND OUTLOOK

We introduce two additive multigrid variants which are conceptually close to AFAC solvers and Mult-additive. An auxiliary term in the equation ensures that overshooting of plain additive multigrid is immediately eliminated. Our results validate that we obtain reasonable performance and stability. They uncover three surprising insights: (i) adAFAC seems to be well-suited to deliver reasonable robustness while solely using geometric inter-grid transfer operators. The construction of good inter-grid



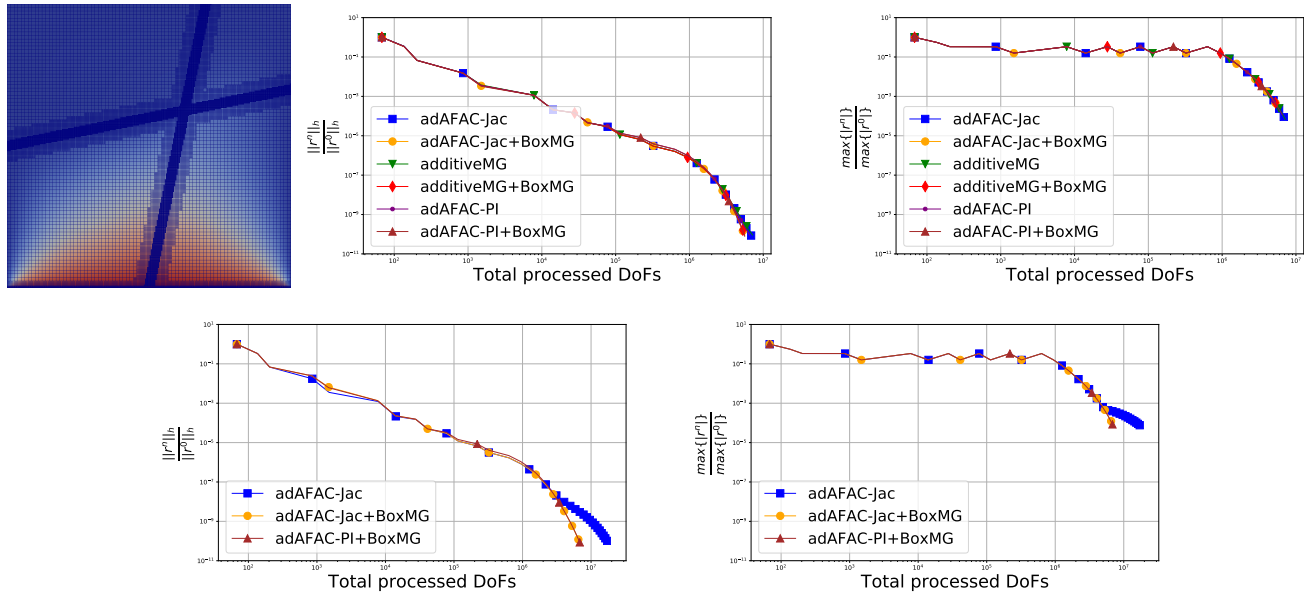


**FIGURE 9** Typical adaptive mesh for a setup where the regions with different material parameter  $\epsilon$  are not axis-aligned. One order of magnitude differences in the material parameter (top) vs. three orders of magnitude (bottom).

transfer operators is far from trivial and computationally cheap. It is thus conceptually an interesting idea to give up on the idea of a good operator and in turn to eliminate oscillations resulting from poor operators within the correction equation. We show that this is a valid strategy for some setups. (ii) adAFAC can be read as an antagonist to BPX. BPX omits the system operator from the correction equations and “solely” relies on proper inter-grid transfer operators. With our geometric adAFAC variants, we work without algebraic operators but a problem-dependent auxiliary smoothing. (iii) BoxMG is a powerful algebraic inter-grid transfer operator construction scheme but cannot compensate for flaws that are introduced by problems that require semicoarsening. Our results do suggest that the auxiliary smoothing might be able to improve the robustness of BoxMG in such scenarios.

It is notoriously difficult to integrate multigrid ideas into existing solvers. Multigrid builds upon several sophisticated building blocks and needs mature, advanced data structures. On the implementation side, an interesting contribution of our work is the simplification and integration of the novel adAFAC idea into well-established concepts. The fusion of three different solves (real solution, hierarchical solution required for HTMG and damping equations) does not introduce any additional implementational complexity compared to standard relaxation strategies. However, it increases the arithmetic intensity. adAFAC can be implemented as single-touch solver on dynamically adaptive grids. This renders it an interesting idea for high performance codes relying on dynamic, flexible meshes.

Studies from a high performance computing point of view are among our next steps. Interest in additive solvers has recently increased as they promise to become a seedcorn for asynchronous algorithms<sup>10</sup>. Our algorithmic sketches integrate all levels’ updates into one grid sweep and thus fall into the class of vertically integrated solvers<sup>5,20</sup>. It will be interesting to study how desynchronisation interplays with the present solver and single-touch ideas. Further, we have to apply the scheme to more realistic, more challenging scenarios. Non-linear equations here are particularly attractive, as our adAFAC implementation already offers a FAS data representation. On the method side, we expect further payoffs by improving the solver components. Notably ideas following<sup>19</sup> which mimic a  $V(1, 1)$ -cycle or even a  $V$ -cycle with more smoothing steps are worth investigating.

## ACKNOWLEDGEMENTS

The authors would like to thank Stephen F. McCormick. Steve read through previous work of the authors<sup>5</sup> and brought up the idea to apply the proposed concepts to AFACx. This kickstarted the present research into an AFAC variant. The authors furthermore would like to thank Thomas Huckle who spotted the elimination of the  $\epsilon$ -dependency in the auxiliary equation.

Finally, the authors thank Edmond Chow for his comments on BPX and for the revitalising of the authors' research on FAC through his own work on asynchronous multigrid.

## References

1. Dongarra J, Hittinger J, et al.. Applied Mathematics Research for Exascale Computing. DOE ASCR Exascale Mathematics Working Group: <http://www.netlib.org/utk/people/JackDongarra/PAPERS/doe-exascale-math-report.pdf>; 2014.
2. Weinzierl T, and Mehl M; SIAM. Peano – A Traversal and Storage Scheme for Octree-Like Adaptive Cartesian Multiscale Grids. *SIAM Journal on Scientific Computing*. 2011;**33**(5):2732–2760.
3. Weinzierl T. The Peano software—parallel, automaton-based, dynamically adaptive grid traversals. *ACM Transactions on Mathematical Software*. 2018;(2nd version under review).
4. Reps B, and Weinzierl T. A Complex Additive Geometric Multigrid Solver for the Helmholtz Equations on Spacetrees. *ACM Transactions on Mathematical Software*. 2017;**44**(1):2:1–2:36.
5. Weinzierl M, and Weinzierl T. Quasi-matrix-free hybrid multigrid on dynamically adaptive Cartesian grids. *ACM Transactions on Mathematical Software*. 2018;(in press).
6. Griebel M. Zur Lösung von Finite-Differenzen-und Finite-Element-Gleichungen mittels der Hierarchischen-Transformations-Mehrgitter-Methode [On the solution of the finite-difference and finite-element equations through the hierarchical-transformational-multigrid method]. Technische Universität München. Institut für Informatik; 1990.
7. Trottenberg U, Oosterlee CW, and Schüller A. Multigrid. Academic Press; 2001.
8. Dendy JE. Black Box Multigrid. *Journal of Computational Physics*. 1982;**48**(3):366–386.
9. Dendy JE, and Moulton JD. Black Box Multigrid with Coarsening by a Factor of Three. *Numerical Linear Algebra with Applications*. 2010;**17**:577–598.
10. Wolfson-Pou J, and Chow E. Asynchronous Multigrid Methods; .
11. Bastian P, Wittum G, and Hackbusch W. Additive and multiplicative multi-grid a comparison. *Computing*. 1998;**60**(4):345–364.
12. McCormick SF, and Thomas J. The fast adaptive composite grid (FAC) method for elliptic equations. *Mathematics of Computation*. 1986;**46**(174):439–456.
13. McCormick SF, and Quinlan DJ. Asynchronous multilevel adaptive methods for solving partial differential equations on multiprocessors: Performance results. *Parallel Computing*. 1989;**12**(2):145–156.
14. Lee B, McCormick SF, Philipp B, and Quinlan DJ. Asynchronous Fast Adaptive Composite-Grid Methods for Elliptic Problems: Theoretical Foundations. *SIAM Journal Numerical Analysis*. 2004;**42**:130–152.
15. Phillip B. 2000. *Elliptic Solvers with Adaptive Mesh Refinement on Complex Geometries*. . Lawrence Livermore National Lab., CA (US).
16. Tuminaro RS, and Tong C. Parallel smoothed aggregation multigrid: Aggregation strategies on massively parallel machines. In: Supercomputing, ACM/IEEE 2000 Conference. IEEE; 2000. p. 5–5.
17. Vaněk P, Mandel J, and Brezina M. Algebraic multigrid by smoothed aggregation for second and fourth order elliptic problems. *Computing*. 1996;**56**(3):179–196.
18. Vaněk P. Fast multigrid solver. *Applications of Mathematics*. 1995;**40**(1):1–20.
19. Vassilevski PS, and Yang UM. Reducing communication in algebraic multigrid using additive variants. *Numerical Linear Algebra with Applications*. 2014;**21**(2):275–296.

20. Adams MF, Brown J, Knepley MG, and Samtaney R. Segmental Refinement: A Multigrid Technique for Data Locality. *SIAM J Scientific Computing*. 2016;**38**(4).
21. Smith B, and P Bjørstad WG. Domain Decomposition—Parallel Multilevel Methods for Elliptic Differential Equations. Cambridge University Press; 1996.
22. Hart L, and McCormick SF. Asynchronous multilevel adaptive methods for solving partial differential equations on multiprocessors: Basic ideas. *Parallel Computing*. 1989;**12**:131–144.
23. Knuth DE. The genesis of attribute grammars. In: Deransart P, and Jourdan M, editors. WAGA: Proceedings of the international conference on Attribute grammars and their applications. Springer-Verlag; 1990. p. 1–12.
24. Brandt A. Multi-level adaptive solutions to boundary-value problems. *Mathematics of Computation*. 1977;**31**(138):333–390.
25. Dubey A, Almgren AS, Bell JB, Berzins M, Brandt SR, Bryan G, et al. A Survey of High Level Frameworks in Block-Structured Adaptive Mesh Refinement Packages. *Journal of Parallel and Distributed Computing*. 2014;**74**(12):3217–3227.
26. Hart L, McCormick SF, and O’Gallagher A. The Fast Adaptive Composite-Grid Method (FAC): Algorithms for Advanced Computers. *Applied Mathematics and Computation*. 1986;p. 103–125.
27. Jimack PK, and Walkley MA. Asynchronous parallel solvers for linear systems arising in computational engineering. *Computational technology reviews*. 2011;**3**:1–20.
28. Rüde U. Multiple tau-extrapolation for multigrid methods. Bibliothek d. Fak. für Mathematik u. Informatik, TUM; 1987.
29. Yavneh I, and Weinzierl M. Nonsymmetric Black Box Multigrid with Coarsening by Three. *Numerical Linear Algebra with Applications*. 2012;**19**(2):246–262.
30. Press WH, and Teukolsky SA. Multigrid Methods for Boundary Value Problems. I. *Computers in Physics*. 1991;**5**(5):514–519.
31. Kouatchou J, and Zhang J. Optimal injection operator and high order schemes for multigrid solution of 3D Poisson equation. *International journal of computer mathematics*. 2000;**76**(2):173–190.
32. Bjørgen J, and Leenaarts J. Numerical non-LTE 3D radiative transfer using a multigrid method. *Astronomy & Astrophysics*. 2017;**599**:A118.
33. Bungartz HJ, and Griebel M. Sparse grids. *Acta Numerica*. 2004;**13**:147–269.
34. Mehl M, Weinzierl T, and Zenger C. A cache-oblivious self-adaptive full multigrid method. *Numerical Linear Algebra with Applications*. 2006;**13**(2–3):275–291.

**How to cite this article:** Charles D Murray, and Tobias Weinzierl (<year>), <journal title>, <journal name> <year> <vol>  
Page <xxx>–<xxx>